Immunity, Vol. 23, 361–374, October, 2005, Copyright ©2005 by Elsevier Inc. DOI 10.1016/j.immuni.2005.09.003

SHIP Represses the Generation of Alternatively Activated Macrophages

Michael J. Rauh,[1] Victor Ho,[1] Carla Pereira,[1,4] Anita Sham,[1] Laura M. Sly,[1] Vivian Lam,[1] Lynsey Huxham,[2] Andrew I. Minchinton,[2] Alice Mui,[3] and Gerald Krystal[1,*]

[1]Terry Fox Laboratory
[2]Department of Medical Biophysics
British Columbia Cancer Agency
Vancouver, British Columbia V5Z 1L3
Canada
[3]Jack Bell Research Centre
Vancouver, British Columbia V6H 3Z6
Canada

Summary

We recently reported that SHIP restrains LPS-induced classical (M1) activation of in vitro differentiated, bone marrow-derived macrophages (BMMΦs) and that SHIP upregulation is essential for endotoxin tolerance. Herein, we show that in vivo differentiated SHIP$^{-/-}$ peritoneal (PMΦs) and alveolar (AMΦs) macrophages, unlike their wild-type counterparts, are profoundly M2 skewed (alternatively activated), possessing constitutively high arginase I (Argl) and Ym1 levels and impaired LPS-induced NO production. Consistent with this, SHIP$^{-/-}$ mice display M2-mediated lung pathology and enhanced tumor implant growth. Interestingly, BMMΦs from SHIP$^{-/-}$ mice do not display this M2 phenotype unless exposed to TGFβ within normal mouse plasma (MP) during in vitro differentiation. Our results suggest that SHIP functions in vivo to repress M2 skewing and that macrophage polarization can occur during differentiation in response to TGFβ if progenitors have elevated PIP_3.

Introduction

Macrophages (MΦs) orchestrate both the initiation and resolution phases of inflammation. The initial inflammatory response is carried out by classically activated (M1) MΦs, which eradicate invading microorganisms and tumor cells and promote type I immune responses, while the resolution phase is carried out by alternatively activated (M2) MΦs, which are hyporesponsive to proinflammatory stimuli and are involved in debris scavenging, angiogenesis, tissue remodeling, wound healing, and the promotion of type II immunity (Gordon, 2003; Mosser, 2003; Stein et al., 1992). Interestingly, MΦs within tumors (tumor-associated macrophages, TAMs) or from patients with severe or chronic inflammation resemble M2 MΦs (Gordon, 2003). In the case of severe/chronic inflammation, this is thought to be an adaptation to avoid damage to the host (Dal Pizzol, 2004; Takahashi et al., 2004). However, in the case of cancer, M2 skewing enables tumors to exploit the healing properties of this subclass of MΦs for tumor growth and immune system evasion (Rodriguez et al., 2004). Despite these observations and the great therapeutic potential of harnessing MΦ polarization, the mechanisms underlying MΦ programming have yet to be fully elucidated. Moreover, it is unresolved whether M1 and M2 MΦs represent distinct, defined lineages, or whether mature MΦ phenotypes are plastic and adaptable to ever-changing environmental cues (Mills et al., 2000; Stout and Suttles, 2004).

We recently demonstrated that the Src homology 2-containing inositol-5′-phosphatase, SHIP, a potent negative regulator of the phosphatidylinositol 3-kinase (PI3K) pathway in hematopoietic cells, restrains lipopolysaccharide (LPS)-induced proinflammatory cytokine and nitric oxide (NO) production from in vitro derived bone marrow macrophages (BMMΦs) (Sly et al., 2004). We also showed that LPS stimulates a 10-fold increase in SHIP protein levels and that this elevation in SHIP plays a critical role in dampening down the effects of a second exposure to LPS (i.e., its upregulation is essential for endotoxin tolerance [Sly et al., 2004]).

To extend the findings that we obtained with in vitro generated BMMΦs, we compared the effects of LPS on primary peritoneal (PMΦs) and alveolar (AMΦs) macrophages from SHIP$^{+/+}$ and –/– mice. In contrast to our results with in vitro derived BMMΦs, we report herein that SHIP$^{-/-}$ PMΦs and AMΦs produce far less NO than their wild-type counterparts because of constitutively elevated levels of arginase I (Argl), which competes with inducible nitric oxide synthase (iNOS) for the common substrate, L-arginine. In addition, we find that in vivo differentiated SHIP$^{-/-}$ MΦs display other features characteristic of an M2 phenotype. However, this M2 skewing is not observed with in vitro derived SHIP$^{-/-}$ BMMΦs unless TGFβ1-containing mouse plasma (MP) is added early to standard in vitro differentiation cultures. Taken together, our results suggest that SHIP$^{-/-}$ MΦs are M2 skewed because of elevated intracellular levels of PIP_3 as well as exposure to extracellular factors during a critical stage in their development.

Results

LPS-Stimulated SHIP$^{-/-}$ PMΦs Secrete Low Levels of NO but Can Be Rescued by Exogenous L-Arginine

In preliminary studies with in vitro generated BMMΦs, we found that LPS stimulated more NO secretion from SHIP$^{-/-}$ than +/+ BMMΦs and that the PI3K inhibitor, LY294002, markedly inhibited this NO production from both cell types (Figure 1A, left). Since we recently showed that LPS-treated SHIP$^{-/-}$ BMMΦs display higher PI3K pathway activation than wild-type BMMΦs (as assessed by higher pAkt levels [Sly et al., 2004]), these results are consistent with the PI3K pathway being a positive regulator of LPS-induced NO production. However, there was no significant difference in the

*Correspondence: gkrystal@bccrc.ca
[4]Present address: StemCell Technologies, Vancouver, British Columbia V5Z 4J7, Canada.

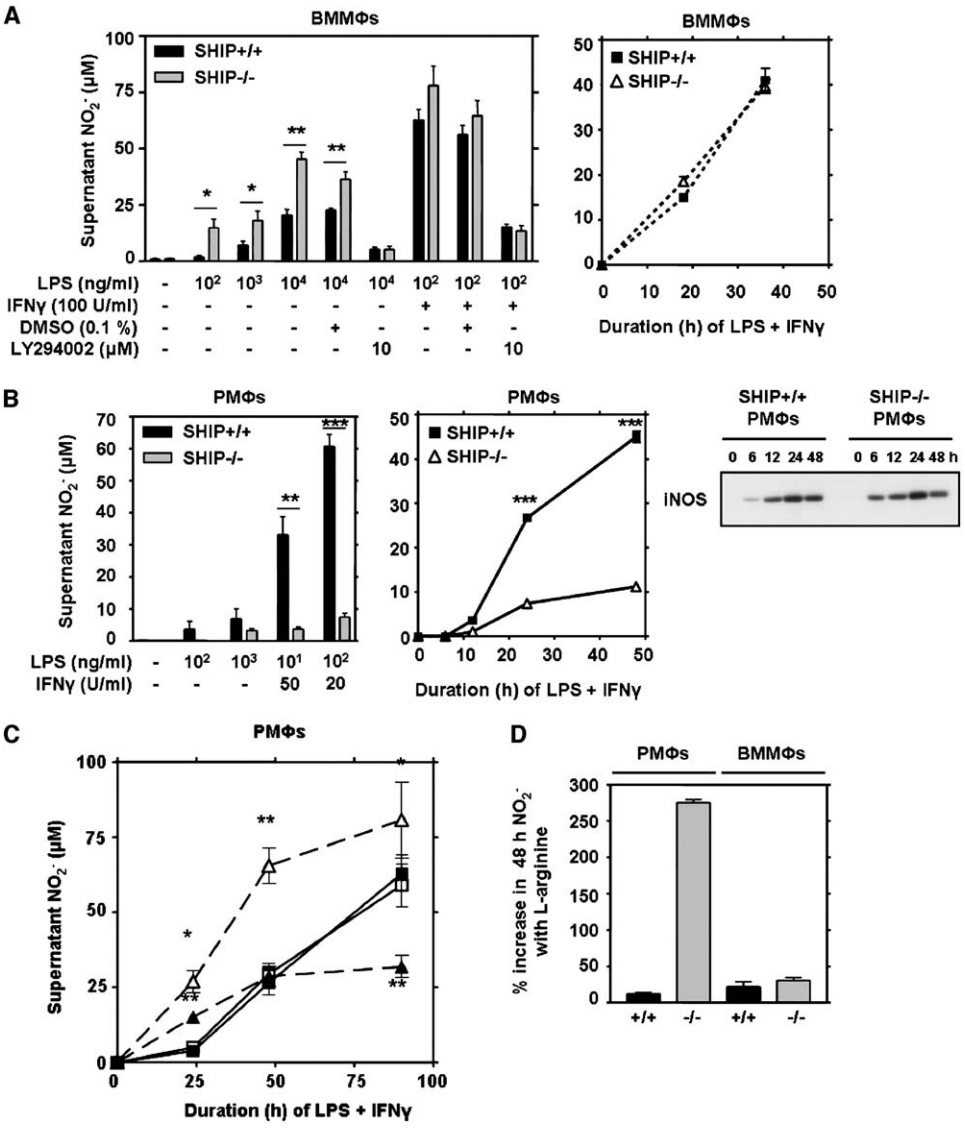

Figure 1. LPS-Stimulated SHIP$^{-/-}$ PMΦs, Unlike BMMΦs, Are Deficient in NO Production due to Limiting L-Arginine

(A) SHIP$^{+/+}$ and –/– BMMΦs (10^6 cells/ml) were treated with LPS ± IFNγ for 24 hr ± prior (30 min) addition of DMSO vehicle or LY294002 (left) or for the indicated times with 100 ng/ml LPS + 20 U/ml IFNγ (right), and the conditioned media were analyzed for nitrite levels.

(B) SHIP$^{+/+}$ and –/– resting (left) or thioglycollate-elicited (middle) PMΦs were treated ± LPS and IFNγ for 24 hr (left) or LPS (100 ng/ml) + IFNγ (20 U/ml) (middle) and NO production measured. Total cell lysates (TCLs) were also prepared from equal numbers of these PMΦs and subjected to Western analysis for iNOS (right).

(C) SHIP$^{+/+}$ (squares) and –/– (triangles) PMΦs were treated with 100 ng/ml LPS + 100 U/ml IFNγ for the indicated times, and NO production was measured with (open symbols) or without (closed symbols) 30 min prior addition of 2 mM L-arginine.

(D) SHIP$^{+/+}$ and –/– PMΦs and BMMΦs were treated for 48 hr with LPS + IFNγ (as in [C]) ± 2 mM L-arginine, and NO production was measured and expressed as % increase in NO of L-arginine supplemented/nonsupplemented controls. Data points in all panels are the means ± SEM of at least triplicate determinations, except for duplicate determinations in (D). Significant difference between SHIP$^{+/+}$ and SHIP$^{-/-}$: *$p < 0.05$, **$p < 0.01$, ***$p < 0.001$, using unpaired two-tailed Student's t test. Similar results were obtained in at least three separate experiments.

amount of NO produced from SHIP$^{+/+}$ and –/– BMMΦs in response to LPS + IFNγ (Figure 1A, left and right). This suggests, perhaps, that the primary effect of the PI3K pathway in LPS-induced BMMΦs is to increase the production of autocrine-acting IFNβ, since addition of exogenous IFNγ would negate this effect. This is consistent with previous studies showing that PI3K positively regulates the translation and/or secretion of IFNβ (Rhee et al., 2003; Weinstein et al., 2000).

Unexpectedly, when we then compared the ability of in vivo differentiated PMΦs from SHIP$^{+/+}$ and –/– mice to produce NO in response to LPS or LPS + IFNγ, we found that the SHIP$^{-/-}$ PMΦs produced far less NO (Figure 1B, left and middle). The cells used to generate the middle panel of Figure 1B were also subjected to Western analysis to determine if LPS+ IFNγ was less efficient at upregulating inducible nitric oxide synthase (iNOS) in SHIP$^{-/-}$ PMΦs. As shown in Figure 1B (right), this was

not the case. Although further studies revealed that LPS-induced iNOS levels were sometimes lower and sometimes higher in LPS-induced SHIP$^{-/-}$ PMΦs, LPS-induced NO was consistently lower in SHIP$^{-/-}$ PMΦs. We then asked if the iNOS substrate, L-arginine, was limiting in SHIP$^{-/-}$ PMΦs by comparing NO production from LPS + IFNγ-stimulated SHIP$^{+/+}$ and –/– PMΦs ± exogenously added 2 mM L-arginine. Of note, the level of L-arginine in IMDM is approximately 400 μM. As shown in Figures 1C and 1D, the addition of L-arginine had a negligible effect on NO production from LPS + IFNγ-stimulated SHIP$^{+/+}$ PMΦs but dramatically increased NO production from SHIP$^{-/-}$ PMΦs. Notably, this effect was not observed with in vitro derived SHIP$^{-/-}$ BMMΦs (Figure 1D).

LPS-Stimulated SHIP$^{-/-}$ PMΦs and AMΦs Secrete Low Levels of NO because of Constitutively High Arginase Activity

To investigate why SHIP$^{-/-}$ PMΦs had inadequate stores of L-arginine for NO synthesis, we noted from the literature that M2 MΦs possess very high levels of arginase I (ArgI) and this effectively competes with iNOS for L-arginine, converting it into urea and ornithine, the latter being metabolized to polyamines and proline to stimulate cell proliferation and collagen formation, respectively (Goerdt and Orfanos, 1999; Gordon, 2003; Mills, 2001). We therefore asked if ArgI was elevated in SHIP$^{-/-}$ PMΦs and found this was indeed the case. Specifically, while the protein levels of ArgI increased slightly in wild-type PMΦs with time following LPS + IFNγ, they were markedly and constitutively elevated in SHIP$^{-/-}$ PMΦs (Figure 2A). To determine if these constitutively elevated ArgI levels in SHIP$^{-/-}$ PMΦs were responsible for the low LPS-induced NO production from these cells, we compared the effects of the arginase inhibitors, L-nor-NOHA and L-norvaline, and found that they significantly increased LPS-induced NO production from SHIP$^{-/-}$ but not +/+ PMΦs (see Figure S1 in the Supplemental Data available with this article online).

ArgI expression is restricted primarily to hepatocytes (where it is expressed in a constitutive fashion to generate urea as part of the urea cycle) and to MΦs (where it is expressed in an inducible fashion) (Wu and Morris, 1998). As shown in Figure 2B, ArgI levels (left) and activity (right) were also dramatically elevated in SHIP$^{-/-}$ AMΦs isolated from bronchoalveolar lavage (BAL). Consistent with this, we found that SHIP$^{-/-}$ produced less NO than SHIP$^{+/+}$ AMΦs in response to LPS + IFNγ (data not shown). However, as shown in Figure 2C, there was no detectable difference in ArgI levels (left) or activity (right) in hepatocyte-rich liver homogenates from SHIP$^{+/+}$ and –/– mice, suggesting that the differences were MΦ specific.

Arginase I Levels Are Upregulated by the PI3K Pathway

To gain some insight into why ArgI levels were elevated in SHIP$^{-/-}$ PMΦs and AMΦs, we stimulated SHIP$^{+/+}$ PMΦs with LPS ± LY294002 or wortmannin and found that these PI3K inhibitors reduced LPS-induced ArgI levels (Figure 2D). We then transiently transfected SHIP$^{+/+}$ PMΦs with a constitutively active PI3K (p110CAAX) and found that it caused a modest, dose-dependent increase in both arginase activity and ArgI levels in the absence of LPS stimulation (Figure 2E). We also subjected SHIP$^{-/-}$ PMΦs to low doses of LY294002 for 48 hr and found that it reduced both arginase activity and ArgI levels (Figure 2F). These results were consistent with PI3K being a positive regulator of ArgI and suggested that the increased PIP_3 levels in SHIP$^{-/-}$ PMΦs were responsible for the increased arginase activity. We then asked if the increased ArgI protein levels in SHIP$^{-/-}$ PMΦs were due, at least in part, to increased transcription and/or stability of ArgI mRNA by carrying out semiquantitative RT-PCR of unstimulated SHIP$^{+/+}$ and –/– PMΦs. As shown in Figure 2G, higher ArgI mRNA levels were present in SHIP$^{-/-}$ PMΦs.

Evidence for SHIP$^{-/-}$ M2 MΦ Skewing In Vivo

To gather evidence for M2 MΦ skewing in vivo, we compared histological sections of lungs from >8-week-old SHIP$^{+/+}$ and –/– mice and found considerable consolidation and fibrosis in the latter (Figure 3A, compare panels 1 and 2). This was consistent with M2-MΦ-induced proliferation (Song et al., 2000) and reminiscent of human T_H2-skewed asthmatic lungs (Zimmermann et al., 2003). Additionally, SHIP$^{-/-}$ lungs and BAL fluids (BALF) revealed the presence of large, hexagonal, MΦ-associated crystals (Figure 3A, panels 3–6). Similar crystals have been reported in the lungs of motheaten viable (MeV) mice, which lack functional tyrosine phosphatase 1 (SHP1), and have been shown in these mice to be composed of the chitinase-like protein, Ym1 (Guo et al., 2000). To determine if MΦs from SHIP$^{-/-}$ mice also express Ym1, we carried out semiquantitative RT-PCR with both PMΦs and AMΦs, and we found that Ym1 mRNA levels were indeed elevated in SHIP$^{-/-}$ MΦs (Figure 3B). To confirm this at the protein level, in the absence of commercially available anti-Ym1, we carried out SDS-PAGE with both cell-free BALF from SHIP$^{+/+}$ and –/– mice and with purified crystals from the BALF of SHIP$^{-/-}$ mice, and we found a prominent 45 kDa Coomassie blue band, corresponding to the molecular mass of Ym1 (Guo et al., 2000; Hung et al., 2002), only in the SHIP$^{-/-}$ fluids and markedly enriched in the crystals from SHIP$^{-/-}$ mice (Figure 3C). Mass spectral analysis of this purified band confirmed that it was Ym1 (Table S1). We then generated a rabbit anti-Ym1 antibody and used it to confirm enhanced expression of Ym1 in SHIP$^{-/-}$ AMΦs and BALF (Figure 3D) and PMΦs (Figure 3E). Cross-reactive bands of 52, 39, and 30 kDa were also elevated in SHIP$^{-/-}$ MΦs and BALF (Figure 3E) and may represent AMCase, chitotriosidase 1, and a breakdown product of Ym1, respectively (Boot et al., 2001; Nio et al., 2004), given the peptide antigen used. Of note, our detecting Ym1 protein in SHIP$^{+/+}$ AMΦs but not PMΦs is consistent with our RT-PCR results (Figure 3B) and confirms a previous report showing that Ym1 is present in wild-type AMΦs (Hung et al., 2002).

Given the presence of M2 MΦs in SHIP$^{-/-}$ mice, we asked if these mice were more amenable to tumor growth (Mantovani et al., 2002; Rodriguez et al., 2004) by subcutaneously injecting M27 Lewis lung carcinoma

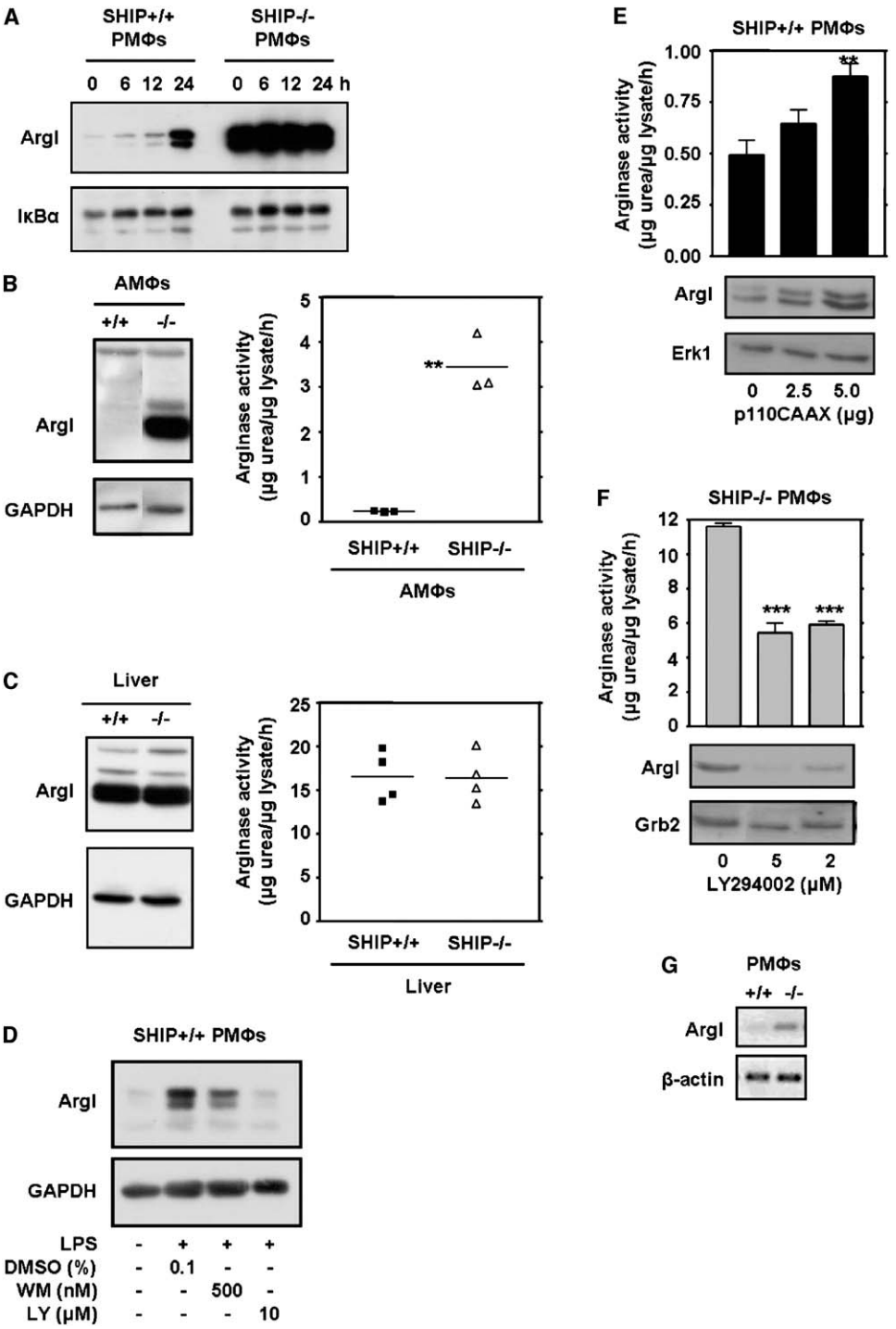

Figure 2. LPS-Stimulated SHIP$^{-/-}$ PMΦs and AMΦs Secrete Low Levels of NO due to Constitutively High Arginase Activity

(A) SHIP$^{+/+}$ and –/– PMΦs (10^6 cells/ml) were stimulated for the indicated times with 100 ng/ml LPS + 20 U/ml IFNγ and TCLs subjected to Western analysis for ArgI and IκBα.

(B) Unstimulated AMΦs isolated from SHIP$^{+/+}$ or –/– BAL fluid by adherence were lysed after overnight incubation and subjected to ArgI and GAPDH Western analysis (left) or arginase activity assays (right) in which the amount of urea produced from the hydrolysis of L-arginine in 1 hr was normalized to the amount of protein in the lysate (**$p < 0.01$).

(C) Liver homogenates, prepared from SHIP$^{+/+}$ and –/– mice in arginase assay lysis buffer, were subjected to ArgI and GAPDH Western analysis (left) and arginase activity assays (right) as in (B).

(D) SHIP$^{+/+}$ PMΦs, pretreated for 30 min with wortmannin, LY294002, or DMSO, were treated ± 200 ng/ml LPS for 24 hr. TCLs from equal numbers of cells were subjected to ArgI and GAPDH Western analysis.

(E and F) SHIP$^{+/+}$ PMΦs (2×10^6 cells/6 cm plate) (E) were transiently transfected with the indicated amount of p110CAAX using DEAE-dextran, allowed to recover overnight, or SHIP$^{-/-}$ PMΦs (F) were incubated for 48 hr with the indicated concentration of LY294002, and lysates prepared for arginase assays (upper panels) or ArgI, Erk1, and Grb2 Western analysis (lower panels).

(G) Total RNA was obtained from SHIP$^{+/+}$ and –/– PMΦs using Trizol and mRNA levels of ArgI and β-actin determined by semiquantitative RT-PCR, using specific primers and after titrating optimal cycle numbers. Results are representative of at least two separate experiments. Bar graphs are the means ± SEM of quadruplicate determinations.

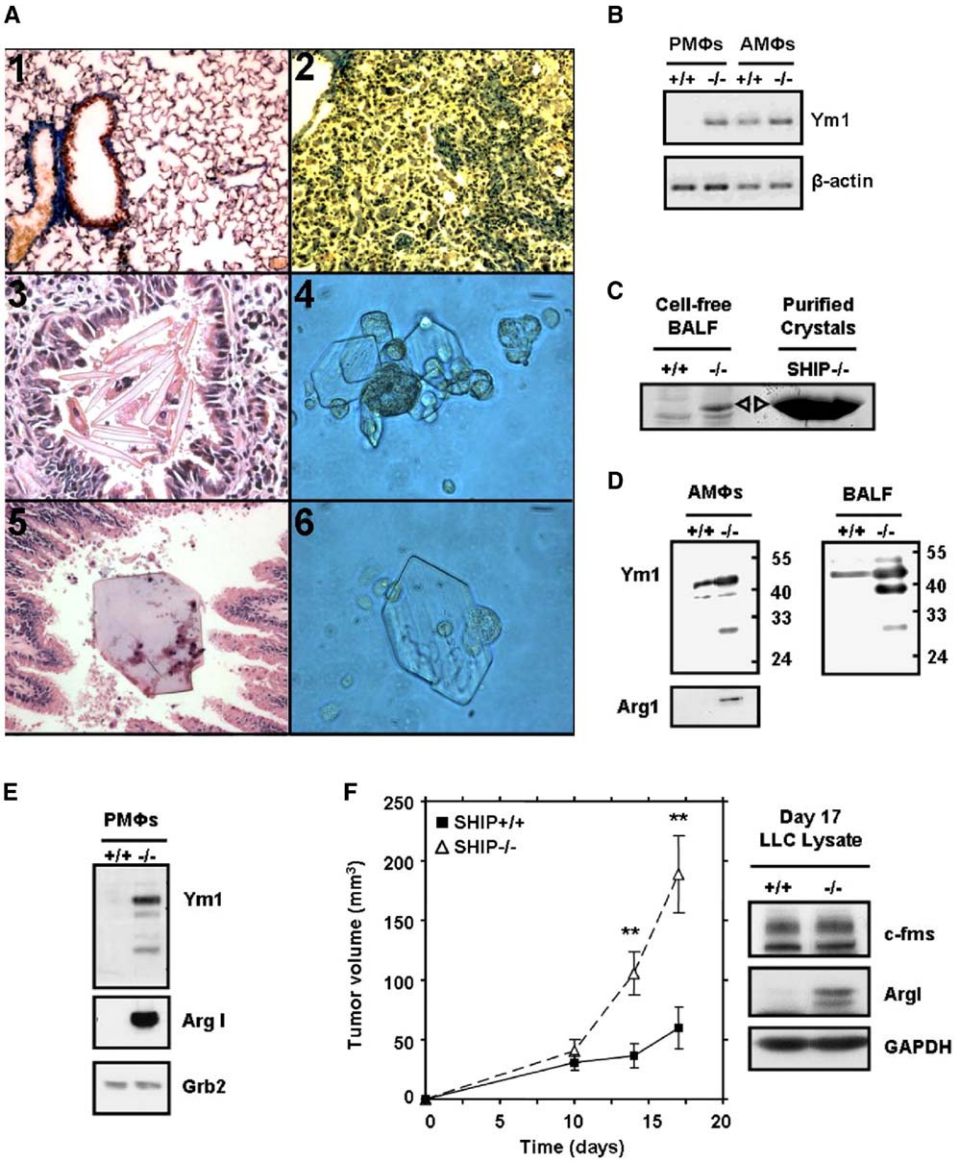

Figure 3. Evidence for SHIP$^{-/-}$ M2 MΦ Skewing In Vivo

(A) Panels 1 and 2 are photomicrographs of Mason trichrome stained histological sections of SHIP$^{+/+}$ (1) and –/– (2) lungs (200×). Panel 3 is a photomicrograph of an H&E-stained SHIP$^{-/-}$ lung histological section revealing a bronchiolar lumen occluded with MΦ-associated, extracellular, eosinophilic crystals. Panel 4 is an image of tissue culture plate-adherent SHIP$^{-/-}$ AMΦs and MΦ-associated crystals. Panel 5 is a photomicrograph of H&E-stained SHIP$^{-/-}$ lung showing a hexagonal, eosinophilic crystal almost occluding a lumen, and panel 6 is a similar MΦ-associated crystal observed in BAL fluid (400× for panels 3–6).

(B) Total RNA was obtained from SHIP$^{+/+}$ and –/– PMΦs or AMΦs and subjected to Ym1 RT-PCR, by use of specific primers and after titrating optimal cycle numbers. β-actin was also optimally titrated as a control.

(C) 40 μg of total BALF protein from SHIP$^{+/+}$ and SHIP$^{-/-}$ mice, together with purified crystals obtained from 3 ml of pooled BALF from SHIP$^{-/-}$ mice by repeated centrifugations through Ficoll-diatrizoate, were boiled for 10 min in SDS-sample buffer and resolved by SDS-PAGE. A 45 kDa Coomassie-stained protein band enriched in SHIP$^{-/-}$ cell-free BALF that comigrated with purified crystals is indicated by an open arrowhead.

(D) Normalized protein equivalents from SHIP$^{+/+}$ and –/– AMΦ lysates, BALF, or PMΦs (E) were subjected to Western analysis using antibodies to Ym1, Argl, and Grb2.

(F) 6- to 10-week-old SHIP$^{+/+}$ (filled squares) (n = 11) and –/– (open triangles) (n = 10) mice were subcutaneously injected with 2 × 10^5 M27 Lewis lung carcinoma cells and tumor volume (mm^3) measured over time (left) (**p < 0.01). Each data point is the mean ± SEM of n. Tumors were also harvested from several mice on day 17, and lysates with equivalent protein levels were subjected to Western analysis for c-fms, Argl, and GAPDH (right).

cells into SHIP$^{+/+}$ and –/– mice. As shown in the left panel of Figure 3F, the tumors grew substantially faster in the SHIP$^{-/-}$ mice. We also analyzed the tumors for their Argl levels and found they were significantly higher in SHIP$^{-/-}$ mice (Figure 3F, right). Related to this, a recent mouse study showed that within subcutane-

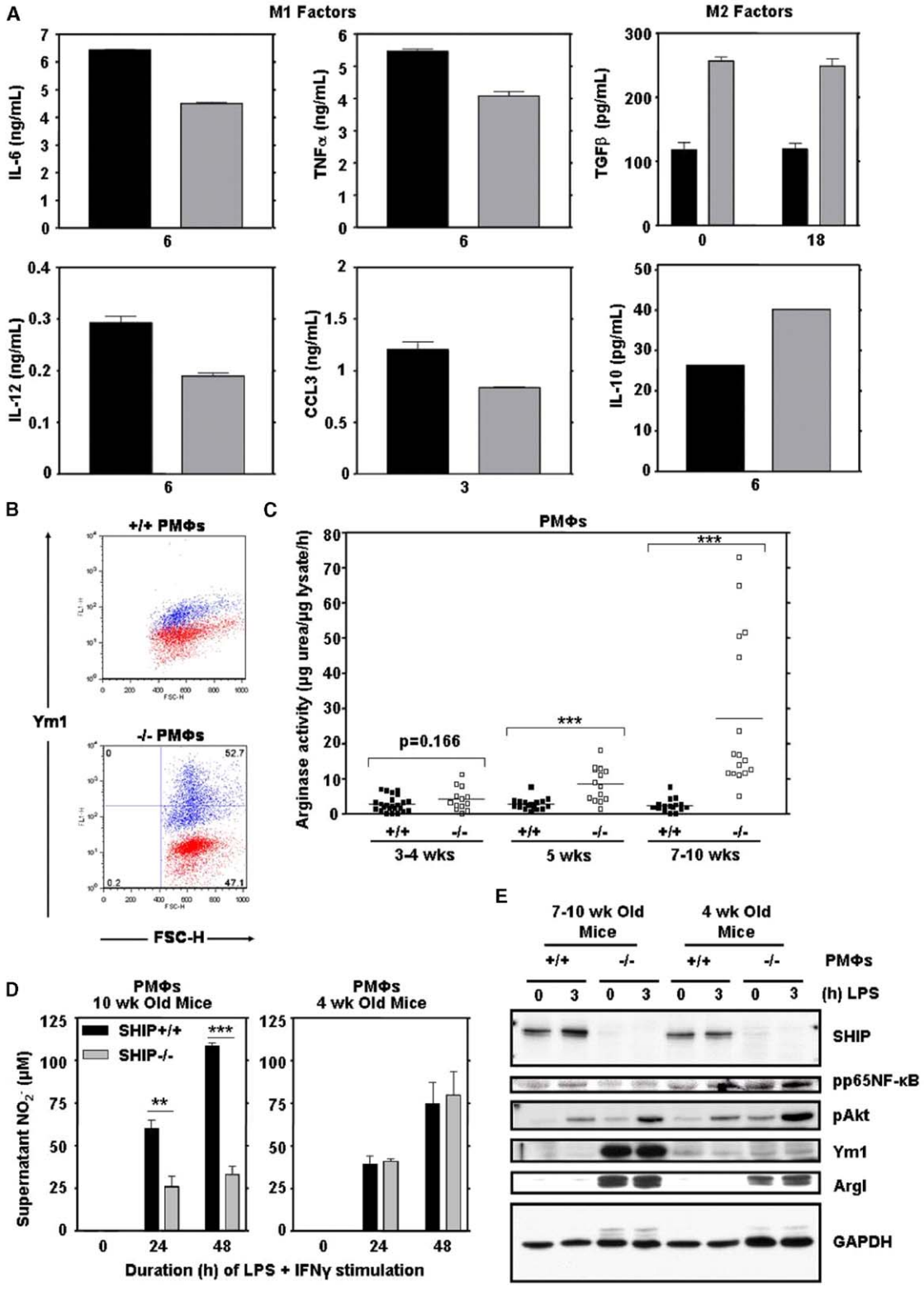

Figure 4. Further Characterization of the SHIP$^{-/-}$ MΦ Phenotype and Its Dependence on Mouse Age

(A) PMΦs from 10-week-old SHIP$^{+/+}$ (black bars) and –/– (gray bars) mice were treated with LPS (100 ng/ml), and the secreted levels of TNFα, IL-6, CCL3, IL-12, or IL-10 were determined by ELISA. The same cells were treated for 18 hr ± LPS (200 ng/ml), and the amount of latent + active TGFβ produced was assessed by ELISA. Data shown are the means ± SEM for triplicate determinations except for IL-10, where data are from single determinations.

(B) Forward by side scatter plots for SHIP$^{+/+}$ (top) and –/– (bottom) PMΦs, selected as per Cook et al. (2003), were intracellularly stained with isotype control (red) or 1/25 anti-Ym1 (blue) using a fix and perm kit (Caltag Lab, Burlingame, CA).

ously injected Lewis lung tumors, ArgI was only expressed in the infiltrating mature macrophages (Rodriguez et al., 2004). Since levels of the M-CSF receptor, c-fms, were equivalent in tumors of both genotypes (Figure 3F), this suggested that enhanced Arg1 levels in SHIP$^{-/-}$ tumors were not simply due to greater numbers of recruited MΦs.

Lastly, consistent with high in vivo arginase activity, SHIP$^{-/-}$ mice displayed reduced plasma L-arginine levels (Figure S2).

Further Characterization of the SHIP$^{-/-}$ MΦ Phenotype and Its Dependence on Mouse Age

To this point, we had characterized SHIP$^{-/-}$ MΦs as M2 based solely on their possessing elevated ArgI and Ym1 and yielding low levels of NO in response to LPS. However, M2 MΦs have been reported to be very heterogeneous (Gordon, 2003; Mantovani et al., 2004) and so to further characterize SHIP$^{-/-}$ MΦs, we investigated other markers associated with an M2 phenotype. Our results suggest that while SHIP$^{+/+}$ and –/– 10-week-old PMΦs express similar cell-surface levels of scavenger receptor A (SR-A) (Figure S3B), Mac1 (CD11b), c-fms, F4/80, and no Gr-1 (data not shown), the SHIP$^{-/-}$ PMΦs constitutively express higher than normal levels of Arg1, Ym1, IL-1Ra, IL-10, IL-6, TGFβ, and mannose receptor and, in response to LPS, higher than normal levels of IL-1Ra, IL-10, and TGFβ but lower levels of TNFα, IL-6, IL-12, CCL3, and NO (Figure 4A, Figures S3 and S5, and data not shown). These findings are consistent with SHIP$^{-/-}$ PMΦs possessing an M2 MΦ phenotype (Mantovani et al., 2004).

We then asked what proportion of PMΦs in SHIP$^{-/-}$ mice display this M2 phenotype, since our Western and ELISA data could not discriminate between a small proportion of cells expressing very high levels of M2 proteins or a large proportion expressing moderately elevated M2 proteins. To do this, we compared FACS profiles of PMΦs using our Ym1 antibody. As shown in Figure 4B, we found that about 50% of the SHIP$^{-/-}$ PMΦs, but none of the wild-type PMΦs, expressed markedly elevated Ym1 levels.

We next examined the stability of the SHIP$^{-/-}$ PMΦ M2 phenotype by incubating these cells ex vivo for 5 days ± M-CSF, IL-12, IFNγ, TNFα, or a media change on day 2 and comparing ArgI, Ym1, and LPS-induced NO levels. As shown in Figure S4A, SHIP$^{-/-}$ PMΦ ArgI expression was relatively stable during the 5 days of in vitro culture unless the medium was changed (Δ), suggesting, perhaps, that an autocrine mechanism was involved in the maintenance of high Arg1. As well, LPS-induced NO production remained undetectable under all in vitro conditions (data not shown). In contrast, intracellular Ym1 expression was not sustained. Thus, while SHIP$^{-/-}$ PMΦ ArgI expression and low NO production is stable ex vivo, the signals required to sustain high Ym1 expression may be present only in vivo. On the other hand, we found that the addition of the T_H2 cytokines, IL-4 and IL-13, induced the expression of ArgI and Ym1 in SHIP$^{+/+}$ PMΦs and maintained/induced them in SHIP$^{-/-}$ PMΦs (Figure S4B).

Using 6- to 10-week-old mice, we found considerable variability in SHIP$^{-/-}$ PMΦ ArgI levels, and a retrospective analysis suggested that PMΦs from older SHIP$^{-/-}$ mice possessed higher ArgI levels. To corroborate this, we examined the arginase activity in PMΦs from SHIP$^{+/+}$ and –/– mice at different ages. We found PMΦs from 3- to 4-week-old SHIP$^{-/-}$ mice possessed, on average, only 1.5-fold more arginase activity than in PMΦs from SHIP$^{+/+}$ mice. However, as the SHIP$^{-/-}$ mice aged, the arginase activity increased dramatically in their PMΦs (on average 3-fold and 12-fold over SHIP$^{+/+}$ PMΦs at 5 weeks and 7–10 weeks, respectively) (Figure 4C). This age-induced ArgI increase in SHIP$^{-/-}$ mice correlated nicely with a reduced ability to produce NO in response to LPS + IFNγ (Figure 4D). Similarly, Ym1 protein levels were relatively normal in PMΦs from 4-week-old SHIP$^{-/-}$ mice but were markedly elevated in PMΦs from 7- to 10-week-old SHIP$^{-/-}$ mice (Figure 4E).

We next compared LPS-induced signaling events in SHIP$^{+/+}$ and –/– PMΦs and found, similar to our previous results with BMMΦs (Sly et al., 2004), that the absence of SHIP resulted in an enhanced LPS-induced phosphorylation of Akt (Figure 4E) (but not of Stat1 or p38 [data not shown]) in PMΦs from both young and old mice. In young SHIP$^{-/-}$mice, where M1 cytokine production was not dramatically impaired (Figure S5), LPS-induced phosphorylation of p65 NF-κB (in the transcriptional activation domain) was indistinguishable from wild-type (Figure 4E). However, LPS-induced p65 phosphorylation was reduced in SHIP$^{-/-}$ PMΦs from adult mice, and this may be related to their more severe M1 impairment. Taken together, these results implicate SHIP in LPS-induced signaling in PMΦs and reveal that the M2 phenotype of SHIP$^{-/-}$ PMΦs is associated with an enhanced ability to activate the PI3K/PIP_3/Akt pathway.

Mouse Plasma Skews the In Vitro Differentiation of SHIP$^{-/-}$ Progenitors toward M2 BMMΦs

Having established that in vivo derived SHIP$^{-/-}$ PMΦs and AMΦs possessed an M2 phenotype, we asked whether MΦs derived from the bone marrow of SHIP$^{-/-}$ mice under standard in vitro culture conditions (i.e., M-CSF + 10% FCS) were also M2 skewed, and we found that this was not the case, i.e., SHIP$^{-/-}$ BMMΦs, like SHIP$^{+/+}$ BMMΦs, possessed undetectable ArgI levels (Figure 5A). This was consistent with our finding

(C) SHIP$^{+/+}$ (solid squares) and –/– (open squares) PMΦ arginase activity was recorded as a function of mouse age (***$p < 0.001$ using unpaired t test with Welch's correction).

(D) LPS (100 ng/ml) + IFNγ (100 U/ml)-induced NO production is compared between PMΦs from 10-week-old (left) and 4-week-old (right) SHIP$^{+/+}$ (black bars) and –/– (gray bars) mice. Data shown are the mean ± SEM of triplicate determinations and similar results were obtained in three separate experiments.

(E) TCLs from 2.5 × 10^5 SHIP$^{+/+}$ and –/– PMΦs from 7- to 10-week-old and 4-week-old mice were treated for 3 hr ± 100 ng/ml LPS and subjected to Western analysis for SHIP, phospho-p65 NF-κB (S536), pAkt (T308), Ym1, ArgI, and GAPDH.

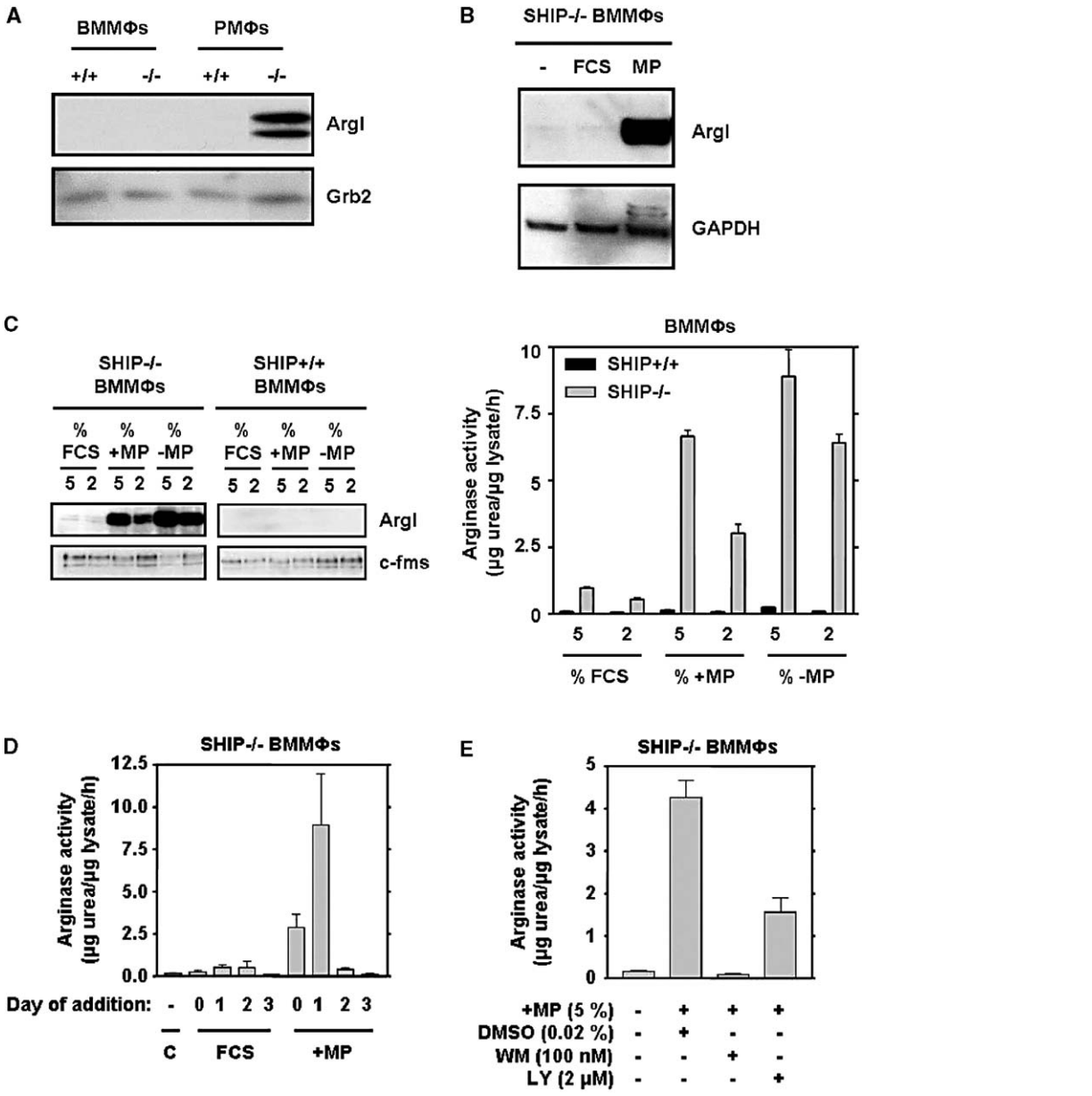

Figure 5. Mouse Plasma Skews the In Vitro Differentiation of SHIP$^{-/-}$ Myelomonocytic Progenitors toward M2 BMMΦs

(A) TCLs (2.5 µg) from SHIP$^{+/+}$ and –/– BMMΦs and PMΦs were subjected to Western analysis using anti-Arg1 and anti-Grb2.

(B) SHIP$^{-/-}$ BMMΦs, generated after 7 days in IMDM + 10% FCS + 5 ng/ml M-CSF (–), + 10% supplemental FCS (FCS), or + 10% +MP (MP), were subjected to Arg1 and GAPDH Western analysis.

(C) In the left panel, SHIP$^{-/-}$ and +/+ bone marrow progenitors were cultured for 7 days in standard differentiation medium ± supplemental FCS, +MP, –MP added 1 day after the initiation of the cultures (i.e., day 1). After 7 days, adherent cells with MΦ morphology were subjected to Arg1 and c-fms (loading control and MΦ differentiation marker) Western analysis. In the right panel, TCLs from (B) were subjected to an arginase assay.

(D) SHIP$^{-/-}$ bone marrow progenitors were cultured as in (B) ± 5% FCS or 5% +MP, added on days 0, 1, 2, or 3, and lysates were assayed for arginase activity as in (C).

(E) SHIP$^{-/-}$ bone marrow progenitors were treated as in (D) except that the day 1 addition of 5% +MP was preceded by a 30 min preincubation with one dose of DMSO, wortmannin, or LY294002, which remained in the medium for the 7 day culture period. Results shown are the mean ± SEM of duplicate determinations. Results are representative of three independent experiments.

that LPS-induced NO production from SHIP$^{-/-}$ BMMΦs was not impaired (Figure 1A) and that L-arginine supplementation did not enhance it (Figure 1D).

In an attempt to mimic the in vivo differentiation environment in SHIP$^{-/-}$ mice, we added 10% mouse plasma (MP) to SHIP$^{-/-}$ in vitro bone marrow cultures and found, after 7 days of culture, that this dramatically increased Arg1 expression (Figure 5B). Supplementation

with an additional 10% FCS, on the other hand, had no effect. We then compared the effect of MP on the in vitro differentiation of SHIP$^{+/+}$ and –/– bone marrow cultures and found that 2% SHIP$^{+/+}$MP (+MP) or SHIP$^{-/-}$ MP (–MP) dramatically increased Arg1 levels (Figure 5C, left) and activity (Figure 5C, right) in the fully developed SHIP$^{-/-}$ BMMΦs, but not +/+ BMMΦs. Additionally, the addition of MP during the in vitro differentiation of SHIP$^{-/-}$ BMMΦs increased the expression of Ym1, TGFβ, and IL-10 and led to a reduced synthesis of M1 markers (TNFα, CCL3, and NO) in response to LPS (data not shown). Thus, the addition of MP successfully mimicked in vivo MΦ differentiation in SHIP$^{+/+}$ and –/– mice and suggested that the in vivo skewing of SHIP$^{-/-}$ MΦs requires both intrinsically elevated PIP_3 levels and an extracellular factor(s) present in the plasma of both genotypes.

To gain some insight into when during differentiation this plasma factor(s) acted, we carried out delayed addition studies with +MP and found that it was no longer capable of inducing high arginase and Ym1 in SHIP$^{-/-}$ BMMΦs if addition was delayed until day 2 (Figure 5D and data not shown). This suggested that it was acting early during MΦ differentiation. Moreover, inclusion of the PI3K inhibitors, wortmannin, or LY294002 with +MP in the 7 day assay diminished arginase induction, suggesting that the plasma factor(s) was dependent upon PI3K for M2 skewing (Figure 5E). Consistent with these in vitro results suggesting that progenitors can become M2 programmed in vivo, we found elevated arginase activity (Figure S6A) and Arg1 (Figure S6B) in peripheral blood monocytes from SHIP$^{-/-}$ mice.

To identify the factor(s) in MP responsible for the upregulation of Arg1 in SHIP$^{-/-}$ MΦ progenitors, we carried out dose-response studies with a number of T_H2-secreted cytokines. Although IL-4, and to a lesser degree, IL-13, were potent inducers of Arg1, they increased Arg1 to the same degree in the resulting SHIP$^{+/+}$ and –/– BMMΦs (Figure 6A). Nonetheless, since wortmannin and LY294002 dampened Arg1 induction by IL-4 in both genotypes, this suggested that the process was still PI3K dependent (Figure S7). IL-6 and GM-CSF, on the other hand, had no effect alone on either cell type (data not shown). Interestingly, TGFβ and IL-10 only induced Arg1 in the resulting SHIP$^{-/-}$ BMMΦs, making them potential candidates for the MP factor (Figure 6A). We therefore preincubated +MP with biotinylated anti-TGFβ1 or biotinylated anti-IL-10, prebound to streptavidin beads, and incubated the depleted plasma samples with SHIP$^{-/-}$ progenitors. As shown in Figure 6B, while this depletion protocol effectively reduced the ability of both exogenously added TGFβ1 and IL-10 to induce arginase activity in the resulting BMMΦs, only TGFβ1 depletion of MP resulted in a reduction (50%) of arginase activity. Thus, TGFβ1 in plasma is at least partially responsible for Arg1 induction in SHIP$^{-/-}$ MΦs. Since –MP was about twice as potent as +MP in Arg1 induction, we asked whether TGFβ levels were elevated in the plasma of SHIP$^{-/-}$ mice, but this was not the case. In fact, TFGβ levels (both total [Figure 6C] and active [data not shown]) were consistently lower in SHIP$^{-/-}$ plasma (Figure 6C). The levels of IL-4, IL-10, IL-12, and IFNγ, on the other hand, were similar in SHIP$^{+/+}$ and –/– mouse plasma and present at very low levels (data not shown). However, SHIP$^{-/-}$ plasma did contain higher IL-6 (Figure 6C) and TNFα (75 pg/ml versus 20 pg/ml in pooled SHIP$^{+/+}$ plasma via cytometric bead array) levels, and it is possible one or both are involved.

Returning to IL-4 and IL-13, which induced arginase equally well in SHIP$^{+/+}$ and –/– bone marrow cultures (Figure 6A), we found that IL-4 (and IL-13, data not shown) could also induce Arg1 in fully mature MΦs (Figure 6D), in keeping with previously published results (Munder et al., 1999; Pauleau et al., 2004), while TGFβ (Jost et al., 2003) or MP could not. We also found, by removing IL-4, IL-13 (data not shown), or MP at different times during the 7 day culture period, that they were all capable of skewing progenitors toward high arginase-expressing mature BMMΦs to some extent, even if they were only present during the first 2 days of culture (Figure 6E). Thus, IL-4 and IL-13 appear capable of M2 skewing both progenitors and mature macrophages.

Discussion

Currently, there is a great deal of controversy concerning the time that M1 and M2 MΦs arise during differentiation and the degree to which these cells can switch phenotypes (Gordon, 2003; Ravasi et al., 2002; Stout and Suttles, 2004). In order to harness these M1 and M2 MΦs for future anticancer and anti-inflammatory therapies, it is very important to resolve these issues. The studies presented herein with SHIP$^{-/-}$ mice provide some unexpected insights into the mechanisms that govern MΦ programming. Specifically, our finding that in vivo derived PMΦs and AMΦs from SHIP$^{-/-}$ mice are M2 programmed while these same cells from SHIP$^{+/+}$ mice have an M1 propensity suggests that SHIP plays a key role in preventing M2 skewing. Additionally, our finding that in vitro derived BMMΦs from SHIP$^{-/-}$ mice are M1 skewed unless exposed to MP during differentiation suggests that extracellular factors play an important role in M1 versus M2 MΦ decisions.

Taken together, our data suggest a model in which elevated PIP_3 levels predispose MΦ progenitors toward an M2 phenotype and SHIP acts as a potent negative regulator of this skewing. In support of this, we found that PI3K inhibitors prevented the induction of Arg1 in SHIP$^{-/-}$ MΦ progenitors by MP (Figure 5E) or TGFβ (data not shown). We also propose that TGFβ and IL-10 can only skew SHIP$^{-/-}$ progenitors to an M2 phenotype because they are weak PI3K-inducers (Bhattacharyya et al., 2004; Kim et al., 2004) and are not known to activate Stat6. In fact, there is growing evidence that, at least in some cell types, TGFβ and IL-10 may actually antagonize the PI3K pathway (Kim et al., 2004; Remy et al., 2004; Sly et al., 2004; Valderrama-Carvajal et al., 2002).

On the other hand, since IL-4 and IL-13 could skew both SHIP$^{+/+}$ and –/– mature MΦs as well as their progenitors toward an M2 phenotype, we propose they can do so because they are not only robust activators of the PI3K pathway (Kelly-Welch et al., 2003; Montaner et al., 1999; Ruetten and Thiemermann 1997) but can activate Stat6 as well (Kelly-Welch et al., 2003; Pauleau et al., 2004). Related to this, we found that PI3K inhibi-

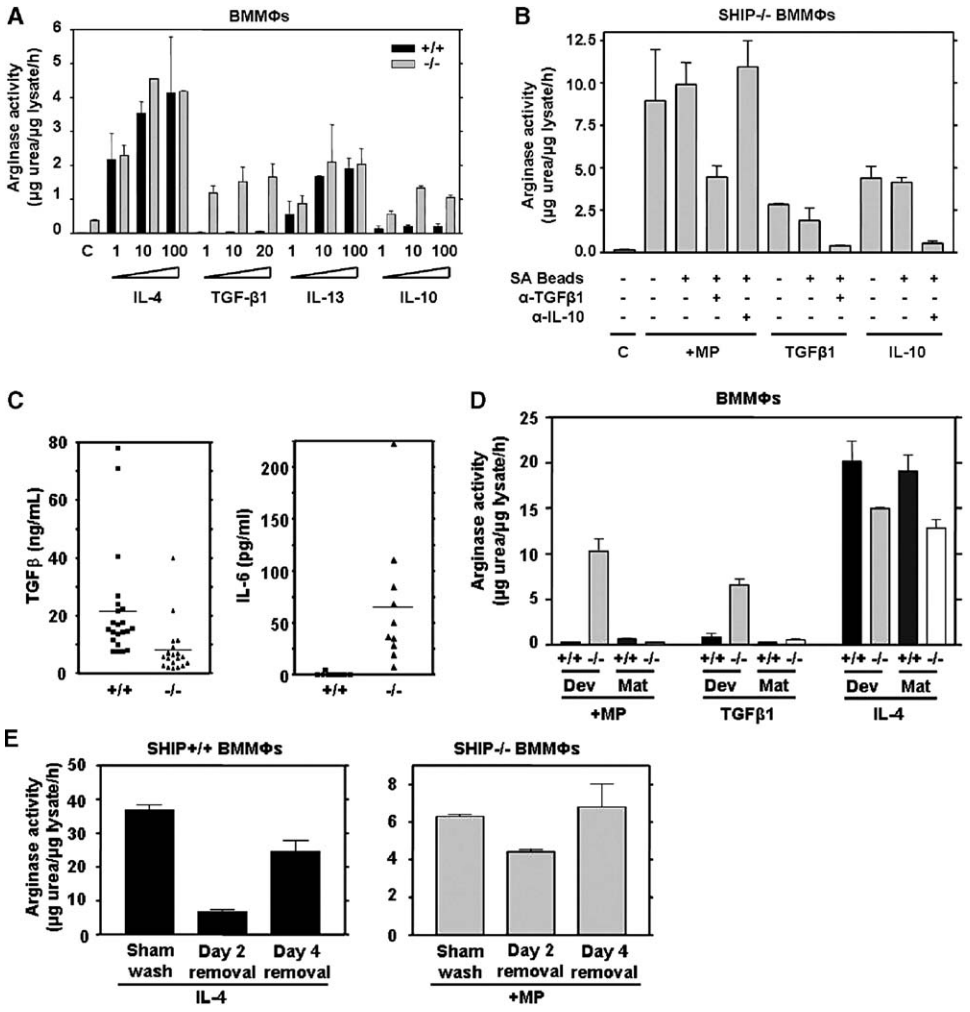

Figure 6. TGFβ and MP Induce Arg1 in Differentiating SHIP$^{-/-}$ BMMΦs

(A) Bone marrow progenitors from SHIP$^{+/+}$ and –/– mice were exposed to T_H2 cytokines at the indicated doses (ng/ml), and arginase activity was measured on day 7.

(B) 50 μg of biotinylated neutralizing chicken anti-mouse TGFβ1 or goat anti-mouse IL-10, at 0.2 mg/ml in PBS, was conjugated to 300 μl SA beads. After washing in PBS to remove unbound antibody, 300 μl aliquots of 5% +MP, 2.5 ng/ml TGFβ1, or 20 ng/ml IL-10 were incubated for 1 hr at 4°C with 100 μl of SA beads alone or antibody-conjugated beads. Suspensions were pulse-centrifuged and the supernatants added to SHIP$^{-/-}$ bone marrow progenitors on day 1. Arginase assays were performed on day 7 as in (A).

(C) Plasma samples from 6- to 10-week-old SHIP$^{+/+}$ and –/– mice were analyzed for TGFβ and IL-6 levels by ELISA.

(D) Bone marrow progenitors (Dev) or mature BMMΦs (Mat) from SHIP$^{+/+}$ and SHIP$^{-/-}$ mice were treated ± 5% +MP or IL-4 (10 ng/ml) for 7 days (Dev) or 3 days (Mat), and arginase activity was determined.

(E) Bone marrow progenitors from SHIP$^{+/+}$ (left) and –/– (right) mice were treated with IL-4 (10 ng/ml) and 5% +MP, respectively, on day 0, and sham washed on day 2, or washed twice and replaced with non-IL-4 or non+MP-containing medium on day 2 or day 4. Arginase assays were performed on day 7. Shown are the means ± SEM of duplicate determinations, and similar results were obtained in two independent experiments.

tors blocked IL-4- and IL-13-induced Arg1 and Ym1 in mature wild-type BMMΦs, without having any significant effect on Stat6 phosphorylation (Figure S8 and data not shown). This suggests that PI3K activation may be a universal requirement for M2 programming, and this may help to explain some of the controversy surrounding the role of PI3K in TLR4 signaling. Thus, although we and others (Rhee et al., 2003; Weinstein et al., 2000) have shown that PI3K can stimulate LPS-induced TLR4 signaling under some circumstances, it also subsequently enhances an anti-inflammatory response.

Our in vitro delayed addition and washing out studies suggest that M2 skewing may occur in vivo in SHIP$^{-/-}$ mice during MΦ differentiation. Consistent with this, we detected elevated Arg1 levels and activity in peripheral blood monocytes from SHIP$^{-/-}$ mice, suggesting that at least some features of M2 programming are attained in SHIP$^{-/-}$ mice prior to terminal differentiation in tissues. Given that MP had only a modest ability to skew SHIP$^{+/+}$ progenitors toward an M2 phenotype in our in vitro differentiation assays, we also tentatively propose that IL-4 and IL-13 do not play a major role in determining M1/M2 MΦ levels in the absence of microbial infec-

tions and that under normal homeostatic conditions, intrinsic PIP_3 levels and TGFβ levels play the dominant role.

With regard to the shift to a more pronounced M2 phenotype with age, previous studies with SHIP$^{-/-}$ mice have shown that natural killer (NK) cells become more tolerant as these mice age, and this prevents them from rejecting mismatched bone marrow grafts (Wang et al., 2002). Moreover, Coggeshall's group recently showed that IL-6 production by SHIP$^{-/-}$ myeloid cells leads to an age-dependent suppression of early B cell development in the bone marrow (Nakamura et al., 2004). Thus, the SHIP$^{-/-}$ mouse may become more tolerant with age and this may be an attempt to counter an environment of chronic inflammation in these mice (Nathan, 2002). This may explain the variability in LPS-induced iNOS levels we observed in SHIP$^{-/-}$ PMΦs, since the lowest levels were observed with cells from the oldest SHIP$^{-/-}$ mice. This is consistent with reports suggesting that the translation of iNOS may be negatively regulated by ArgI-mediated L-arginine depletion and/or polyamine production (Bussiere et al., 2005; El Gayar et al., 2003; Lee et al., 2003). Related to this, both the PI3K pathway and M2 MΦs have been implicated in the compensatory anti-inflammatory response (CARS) (Bone, 1996) observed in septic patients (Learn et al., 2001; Williams et al., 2004), in noninfectious systemic inflammatory response syndrome (SIRS), and in the susceptibility of hosts to nosocomial infections (Adib-Conquy et al., 2003; Takahashi et al., 2004).

One in vivo consequence of enhanced M2 MΦ programming is likely the presence of fibrosis and Ym1 crystals in the lungs of SHIP$^{-/-}$ mice. Ym1 is a chitinase-like secretory lectin that spontaneously crystallizes under high concentrations (e.g., in chronic T_H2-type inflammation like asthma or parasitic infections), particularly in the lung, is associated with the presence of M2 MΦs (Nair et al., 2003; Raes et al., 2002; Welch et al., 2002) and has been postulated to function in myelopoiesis (Hung et al., 2002) and allergic lung remodeling (Hung et al., 2002; Webb et al., 2001). Interestingly, Ym1 lung crystals have also been isolated from MeV mice (Guo et al., 2000), which share many phenotypic characteristics with SHIP$^{-/-}$ mice (Shultz et al., 1993; Tsui et al., 1993), including chronic lung inflammation (Helgason et al., 1998; Ward, 1978). These crystals may represent an exaggerated manifestation of immune tolerance and healing and may, in fact, contribute to the lung pathology in both mouse types. Taken together, our results suggest that MΦs within SHIP$^{-/-}$, and perhaps MeV, mice become constitutively M2 programmed and that this contributes to their lung pathology and shortened life span.

In summary, while most studies on MΦ programming thus far have been conducted with naive, in vitro differentiated, mature BMMΦs, our studies with SHIP$^{-/-}$ progenitors have revealed that the combination of intrinsic (i.e., elevated PIP_3 levels) and extrinsic (i.e., cytokine environment) factors during MΦ differentiation can determine the MΦ phenotype. Naive, mature MΦs can be M2 skewed by factors such as IL-4 and IL-13, and this suggests that the MΦ phenotype can arise both during differentiation and once it is completed. Importantly, our studies have also revealed the requirement for the PI3K pathway during M2 MΦ differentiation and mature activation. Although our studies do not distinguish between distinct M1 and M2 progenitors or a plastic common progenitor, this in vitro system may more accurately reflect the conditions of in vivo MΦ differentiation and programming and be amenable to future studies. Importantly, our studies caution against extrapolating findings obtained with in vitro derived BMMΦs to more complex and dynamic in vivo systems. Finally, we suggest that targeting the SHIP/PI3K axis in situ, or ex vivo, may represent a viable future means of harnessing and manipulating the macrophage phenotype for cancer, infection, and chronic inflammation therapies.

Experimental Procedures

LPS, Cytokines, Reagents, and Antibodies

E. coli LPS from serotype O127:B8 was from the Sigma Chemical Company (St. Louis, MO). The cytokines IFNγ, IL-4, IL-6, IL-10, IL-13, TGFβ1, GM-CSF, and M-CSF were from StemCell Technologies (Vancouver, BC, Canada). The PI3K inhibitors LY294002 and wortmannin were from Calbiochem (La Jolla, CA), while L-nor-NOHA and L-nor-valine were from Alexis Biochem (USA) and Sigma, respectively. The following polyclonal rabbit antibodies were used: iNOS, IκBα, Grb2, and c-fms (Santa Cruz), ERK1 (Stressgen), pStat6, pp65 (S536), pAkt (T308) (Cell Signaling), SHIP (Damen et al., 1998), and Ym1 (generated and affinity purified using the peptide sequence GYTGENSPLYK). Mouse monoclonal antibodies were used to detect ArgI (BD Transduction) and GAPDH (Research Diagnostics). Biotinylated neutralizing chicken anti-mouse TGFβ1 and goat anti-mouse IL-10 were from R&D Systems, and 50 μg of each, reconstituted at 0.2 mg/ml in PBS, were conjugated to 300 μl streptavidin-agarose (SA) beads (Pierce) according to the manufacturer's instructions.

Tissue Culture

BMMΦs and PMΦs were obtained from SHIP$^{+/+}$ and SHIP$^{-/-}$ mice as described previously (Sly et al., 2004). For AMΦs, 0.8 ml prewarmed PBS was injected into the lungs of euthanized mice via the trachea with a 22G needle and a 1 ml syringe (Becton Dickson) and retrieved as BALF. The collected BALF (2–3 washes) was centrifuged at 300 × g and the cells resuspended with 1–2 ml of PMΦ medium and plated in 12-well plates. AMΦs were selected by adherence after repeated washings. For in vitro experiments to mimic the in vivo environment of MΦ differentiation, bone marrow progenitor cells were cultured for 7 days in BMMΦ medium, without medium change, at 0.5–2.0 × 10^6 cells/ml in 24-well plates ± cytokines or MP.

Nitric Oxide Assay

NO production was determined indirectly by measuring the accumulation of the stable end product, NO_2^-, in the tissue culture supernatant using the Griess reaction, as described previously (Sly et al., 2004).

Arginase Assay

Arginase activity was assessed indirectly by measuring the concentration of urea generated by the arginase-dependent hydrolysis of L-arginine, as described (Morrison and Correll, 2002).

ELISAs

Tissue culture supernatants of resting or stimulated MΦs were assessed for protein levels of TNFα, IL-6, CCL3, IL-10, and IL-12 by ELISA (BD Biosciences, Mississauga, ON, Canada) according to the manufacturer's instructions. For mouse plasma analysis, a FACS-based cytometric bead array IL-6, IL-10, IL-12, TNFα, IFNγ, and CCL2/MCP-1 Mouse Inflammation ELISA kit (BD Biosciences) was used according to the manufacturer's instructions. Latent + active TGFβ was assessed in mouse plasma and supernatants by

ELISA (R&D Systems) with the background contribution from 10% FCS subtracted.

Cell Lysis and Western Analysis

MΦs were either lysed directly into 1×SDS sample buffer or into arginase assay buffer. For the latter, protein levels were determined by Bradford assay and samples supplemented with concentrated SDS sample buffer to give 1×SDS sample buffer. All samples were then boiled for 5 min and subjected to Western analysis as described previously (Sly et al., 2004).

Lung Crystal Isolation and Mass Spectroscopy Analysis

Crystals were purified from the lungs of SHIP$^{-/-}$ mice as previously described for MeV mice (Guo et al., 2000), boiled for 5 min in 1×SDS sample buffer, and subjected to SDS-PAGE, along with cell-free BALF from SHIP$^{+/+}$ and –/– mice. The purified 45 kDa band was excised and subjected to in-gel trypsin digestion and subsequent MALDI-TOF MS and ESI MS/MS at the UBC Laboratory of Molecular Biophysics Proteomics Core Facility (Vancouver, BC, Canada).

Lung Histology and BAL Analysis

Lungs were collected from SHIP$^{+/+}$ and –/– mice, formalin fixed, ethanol washed, and paraffin embedded. Lung sections were obtained and stained with MSB or H&E, using standard techniques. Photomicrographs of stained histological sections or BALF and cells were obtained using a QImaging QICAM Fast 1394 Cooled Color 12-bit digit camera mounted on a Leica DMIL microscope, at 200× or 400× original magnification.

RNA Preparation, RPA, and RT-PCR

RNA was isolated as described previously (Sly et al., 2004). RPA of cytokine mRNA levels was performed on 2–10 μg of total RNA using the RiboquantTM Multi-Probe RPA (BD Pharmingen) and template sets mCK2 as described previously (Kalesnikoff et al., 2002). PCR reactions were carried out using previously described primers and conditions specific for ArgI and β-actin (Morrison and Correll, 2002) and Ym1 (Nair et al., 2003), but cycle numbers were optimized for our own laboratory. Negative controls were minus reverse transcriptase and minus template. Black-white inverted images of PCR bands were obtained using a Kodak Digital Science DC40 Camera mounted to a Fisher Biotechnology Transilluminator.

Transient Transfections

SHIP$^{+/+}$ PMΦs were seeded at 2 × 10^6 cells/6 cm plate and transiently transfected using DEAE-Dextran. In brief, 0, 2.5, or 5 μg of a vector containing constitutively active PI3K (pSG5-mycT-p110αCAAX from Drs. J. Downward and S. Wennstrom [Jimenez et al., 1998]) was incubated with DEAE-dextran, at 0.5 mg/ml, in 3 ml IMDM-0.5×PBS for 15 min at 23°C. After two cell washes in IMDM, the DNA/DEAE-dextran mixture was added for 15 min at 23°C. After aspiration, cells were washed once with IMDM and placed in PMΦ medium overnight. The following day, cells were lysed for arginase assays and Western analyses as described above.

Murine Tumor Model

6- to 10-week-old SHIP$^{+/+}$ and –/– mice were subcutaneously injected with 2 × 10^5 M27 Lewis lung carcinoma cells and tumor volume (mm^3) determined over time using calipers and the formula for volume of an ellipsoid. Tumors were also harvested from several mice at day 17 and minced into tiny pieces with scissors, and protein lysates were prepared by homogenizing the tissue in 0.5% NP-40 detergent in PSB plus protease inhibitors, using a syringe and progressively higher gauge needles (Damen et al., 1998). Equivalent protein amounts were then subjected to Western blot analysis for ArgI, c-fms, and GAPDH.

Statistical Analysis

Unpaired, two-tailed Student's t tests were performed where indicated, using GraphPad Prism version 3.02 (GraphPad Software Incorporated).

Supplemental Data

Supplemental Data include eight figures and one table and can be found with this article online at http://www.immunity.com/cgi/content/full/23/4/361/DC1/.

Acknowledgments

We would like to thank Christine Kelly for typing the manuscript, Julie Chow for histology, and Dr. Suzanne Perry for mass spectrometric analysis. M.J.R. would like to thank Drs. J. Damen, C. Helgason, P. Correll, W.J. Murphy, M. Huber, M. Modelell, and Z. Zhu for helpful discussions. This work was supported by the National Cancer Institute of Canada, with funds from the Terry Fox Foundation and core support from both the BC Cancer Foundation and the BC Cancer Agency. M.J.R. holds a Canadian Institutes of Health Research MD/PhD Studentship and a Michael Smith Foundation for Health Research Trainee Incentive Award. L.M.S. holds a Leukemia Research Fund of Canada Fellowship. The authors declare that they have no competing financial interests.

Received: February 20, 2005
Revised: February 20, 2005
Accepted: September 7, 2005
Published: October 18, 2005

References

Adib-Conquy, M., Moine, P., Asehnoune, K., Edouard, A., Espevik, T., Miyake, K., Werts, C., and Cavaillon, J.M. (2003). Toll-like receptor-mediated tumor necrosis factor and interleukin-10 production differ during systemic inflammation. Am. J. Respir. Crit. Care Med. *168*, 158–164.

Bhattacharyya, S., Sen, P., Wallet, M., Long, B., Baldwin, A.S., Jr., and Tisch, R. (2004). Immunoregulation of dendritic cells by IL-10 is mediated through suppression of the PI3K/Akt pathway and of IκB kinase activity. Blood *104*, 1100–1109.

Bone, R.C. (1996). Sir Isaac Newton, sepsis, SIRS, and CARS. Crit. Care Med. *24*, 1125–1128.

Boot, R.G., Blommaart, E.F., Swart, E., Ghauharali-van der Vlugt, K., Bijl, N., Moe, C., Place, A., and Aerts, J.M. (2001). Identification of a novel acidic mammalian chitinase distinct from chitotriosidase. J. Biol. Chem. *276*, 6770–6778.

Bussiere, F.I., Chaturvedi, R., Cheng, Y., Gobert, A.P., Asim, M., Blumberg, D.R., Xu, H., Kim, P.Y., Hacker, A., Casero, R.A., Jr., and Wilson, K.T. (2005). Spermine causes loss of innate immune response to *Helicobacter pylori* by inhibition of inducible nitric-oxide synthase translation. J. Biol. Chem. *280*, 2409–2412.

Cook, A.D., Braine, E.L., and Hamilton, J.A. (2003). The phenotype of inflammatory macrophages is stimulus dependent: implications for the nature of the inflammatory response. J. Immunol. *171*, 4816–4823.

Dal Pizzol, F. (2004). Alternative activated macrophage: a new key for systemic inflammatory response syndrome and sepsis treatment? Crit. Care Med. *32*, 1971–1972.

Damen, J.E., Liu, L., Ware, M.D., Ermolaeva, M., Majerus, P.W., and Krystal, G. (1998). Multiple forms of SHIP are generated by C-terminal truncation. Blood *92*, 1199–1205.

El Gayar, S., Thuring-Nahler, H., Pfeilschifter, J., Rollinghoff, M., and Bogdan, C. (2003). Translational control of inducible nitric oxide synthase by IL-13 and arginine availability in inflammatory macrophages. J. Immunol. *171*, 4561–4568.

Goerdt, S., and Orfanos, C.E. (1999). Other functions, other genes: alternative activation of antigen-presenting cells. Immunity *10*, 137–142.

Gordon, S. (2003). Alternative activation of macrophages. Nat. Rev. Immunol. *3*, 23–35.

Guo, L., Johnson, R.S., and Schuh, J.C. (2000). Biochemical characterization of endogenously formed eosinophilic crystals in the lungs of mice. J. Biol. Chem. *275*, 8032–8037.

Helgason, C.D., Damen, J.E., Rosten, P., Grewal, R., Sorensen, P.,

Chappel, S.M., Borowski, A., Jirik, F., Krystal, G., and Humphries, R.K. (1998). Targeted disruption of SHIP leads to hemopoietic perturbations, lung pathology, and a shortened life span. Genes Dev. *12*, 1610–1620.

Hung, S.I., Chang, A.C., Kato, I., and Chang, N.C. (2002). Transient expression of Ym1, a heparin-binding lectin, during developmental hematopoiesis and inflammation. J. Leukoc. Biol. *72*, 72–82.

Jimenez, C., Jones, D.R., Rodriguez-Viciana, P., Gonzalez-Garcia, A., Leonardo, E., Wennstrom, S., von Kobbe, C., Toran, J.L., Borlado, L., Calvo, V., et al. (1998). Identification and characterization of a new oncogene derived from the regulatory subunit of phosphoinositide 3-kinase. EMBO J. *17*, 743–753.

Jost, M.M., Ninci, E., Meder, B., Kempf, C., Van Royen, N., Hua, J., Berger, B., Hoefer, I., Modolell, M., and Buschmann, I. (2003). Divergent effects of GM-CSF and TGFβ1 on bone marrow-derived macrophage arginase-1 activity, MCP-1 expression, and matrix metalloproteinase-12: a potential role during arteriogenesis. FASEB J. *17*, 2281–2283.

Kalesnikoff, J., Baur, N., Leitges, M., Hughes, M.R., Damen, J.E., Huber, M., and Krystal, G. (2002). SHIP negatively regulates IgE+ antigen-induced IL-6 production in mast cells by inhibiting NFκB activity. J. Immunol. *168*, 4737–4746.

Kelly-Welch, A.E., Hanson, E.M., Boothby, M.R., and Keegan, A.D. (2003). Interleukin-4 and interleukin-13 signaling connections maps. Science *300*, 1527–1528.

Kim, W.K., Hwang, S.Y., Oh, E.S., Piao, H.Z., Kim, K.W., and Han, I.O. (2004). TGF-β1 represses activation and resultant death of microglia via inhibition of phosphatidylinositol 3-kinase activity. J. Immunol. *172*, 7015–7023.

Learn, C.A., Boger, M.S., Li, L., and McCall, C.E. (2001). The phosphatidylinositol 3-kinase pathway selectively controls sIL-1RA not interleukin-1β production in the septic leukocytes. J. Biol. Chem. *276*, 20234–20239.

Lee, J., Ryu, H., Ferrante, R.J., Morris, S.M., Jr., and Ratan, R.R. (2003). Translational control of inducible nitric oxide synthase expression by arginine can explain the arginine paradox. Proc. Natl. Acad. Sci. USA *100*, 4843–4848.

Mantovani, A., Sozzani, S., Locati, M., Allavena, P., and Sica, A. (2002). Macrophage polarization: tumor-associated macrophages as a paradigm for polarized M2 mononuclear phagocytes. Trends Immunol. *23*, 549–555.

Mantovani, A., Sica, A., Sozzani, S., Allavena, P., Vecchi, A., and Locati, M. (2004). The chemokine system in diverse forms of macrophage activation and polarization. Trends Immunol. *25*, 677–686.

Mills, C.D. (2001). Macrophage arginine metabolism to ornithine/urea or nitric oxide/citrulline: a life or death issue. Crit. Rev. Immunol. *21*, 399–425.

Mills, C.D., Kincaid, K., Alt, J.M., Heilman, M.J., and Hill, A.M. (2000). M-1/M-2 macrophages and the Th1/Th2 paradigm. J. Immunol. *164*, 6166–6173.

Montaner, L.J., da Silva, R.P., Sun, J., Sutterwala, S., Hollinshead, M., Vaux, D., and Gordon, S. (1999). Type 1 and type 2 cytokine regulation of macrophage endocytosis: differential activation by IL-4/IL-13 as opposed to IFN-γ or IL-10. J. Immunol. *162*, 4606–4613.

Morrison, A.C., and Correll, P.H. (2002). Activation of the stem cell-derived tyrosine kinase/RON receptor tyrosine kinase by macrophage-stimulating protein results in the induction of arginase activity in murine peritoneal macrophages. J. Immunol. *168*, 853–860.

Mosser, D.M. (2003). The many faces of macrophage activation. J. Leukoc. Biol. *73*, 209–212.

Munder, M., Eichmann, K., Moran, J.M., Centeno, F., Soler, G., and Modolell, M. (1999). Th1/Th2-regulated expression of arginase isoforms in murine macrophages and dendritic cells. J. Immunol. *163*, 3771–3777.

Nair, M.G., Cochrane, D.W., and Allen, J.E. (2003). Macrophages in chronic type 2 inflammation have a novel phenotype characterized by the abundant expression of *Ym1* and *Fizz1* that can be partly replicated in vitro. Immunol. Lett. *85*, 173–180.

Nakamura, K., Kouro, T., Kincade, P.W., Malykhin, A., Maeda, K., and Coggeshall, K.M. (2004). Src homology 2-containing 5-inositol phosphatase (SHIP) suppresses an early stage of lymphoid cell development through elevated interleukin-6 production by myeloid cells in bone marrow. J. Exp. Med. *199*, 243–254.

Nathan, C. (2002). Points of control in inflammation. Nature *420*, 846–852.

Nio, J., Fujimoto, W., Konno, A., Kon, Y., Owhashi, M., and Iwanaga, T. (2004). Cellular expression of murine Ym1 and Ym2, chitinase family proteins, as revealed by in situ hybridization and immunohistochemistry. Histochem. Cell Biol. *121*, 473–482.

Pauleau, A.L., Rutschman, R., Lang, R., Pernis, A., Watowich, S.S., and Murray, P.J. (2004). Enhancer-mediated control of macrophage-specific arginase I expression. J. Immunol. *172*, 7565–7573.

Raes, G., De Baetselier, P., Noel, W., Beschin, A., Brombacher, F., and Hassanzadeh, G.G. (2002). Differential expression of FIZZ1 and Ym1 in alternatively versus classically activated macrophages. J. Leukoc. Biol. *71*, 597–602.

Ravasi, T., Wells, C., Forest, A., Underhill, D.M., Wainwright, B.J., Aderem, A., Grimmond, S., and Hume, D.A. (2002). Generation of diversity in the innate immune system: macrophage heterogeneity arises from gene-autonomous transcriptional probability of individual inducible genes. J. Immunol. *168*, 44–50.

Remy, I., Montmarquette, A., and Michnick, S.W. (2004). PKB/Akt modulates TGF-β signalling through a direct interaction with $Smad_3$. Nat. Cell Biol. *6*, 358–365.

Rhee, S.H., Jones, B.W., Toshchakov, V., Vogel, S.N., and Fenton, M.J. (2003). Toll-like receptor 2 and 4 activate STAT1 serine phosphorylation by distinct mechanisms in macrophages. J. Biol. Chem. *278*, 22506–22512.

Rodriguez, P.C., Quiceno, D.G., Zabaleta, J., Ortiz, B., Zea, A.H., Piazuelo, M.B., Delgado, A., Correa, P., Brayer, J., Sotomayor, E.M., et al. (2004). Arginase I production in the tumor microenvironment by mature myeloid cells inhibits T-cell receptor expression and antigen-specific T-cell responses. Cancer Res. *64*, 5839–5849.

Ruetten, H., and Thiemermann, C. (1997). Interleukin-13 is a more potent inhibitor of the expression of inducible nitric oxide synthase in smooth muscle cells than in macrophages: a comparison with interleukin-4 and interleukin-10. Shock *8*, 409–414.

Shultz, L.D., Schweitzer, P.A., Rajan, T.V., Yi, T., Ihle, J.N., Matthews, R.J., Thomas, M.L., and Beier, D.R. (1993). Mutations at the murine motheaten locus are within the hematopoietic cell protein-tyrosine phosphatase (*Hcph*) gene. Cell *73*, 1445–1454.

Sly, L.M., Rauh, M.J., Kalesnikoff, J., Song, C.H., and Krystal, G. (2004). LPS-induced upregulation of SHIP is essential for endotoxin tolerance. Immunity *21*, 227–239.

Song, E., Ouyang, N., Horbelt, M., Antus, B., Wang, M., and Exton, M.S. (2000). Influence of alternatively and classically activated macrophages on fibrogenic activities of human fibroblasts. Cell. Immunol. *204*, 19–28.

Stein, M., Keshav, S., Harris, N., and Gordon, S. (1992). Interleukin 4 potently enhances murine macrophage mannose receptor activity: a marker of alternative immunologic macrophage activation. J. Exp. Med. *176*, 287–292.

Stout, R.D., and Suttles, J. (2004). Functional plasticity of macrophages: reversible adaptation to changing microenvironments. J. Leukoc. Biol. *76*, 1–5.

Takahashi, H., Tsuda, Y., Takeuchi, D., Kobayashi, M., Herndon, D.N., and Suzuki, F. (2004). Influence of systemic inflammatory response syndrome on host resistance against bacterial infections. Crit. Care Med. *32*, 1879–1885.

Tsui, H.W., Siminovitch, K.A., de Souza, L., and Tsui, F.W. (1993). *Motheaten* and *viable motheaten* mice have mutations in the haematopoietic cell phosphatase gene. Nat. Genet. *4*, 124–129.

Valderrama-Carvajal, H., Cocolakis, E., Lacerte, A., Lee, E.H., Krystal, G., Ali, S., and Lebrun, J.J. (2002). Activin/TGF-β induce apoptosis through Smad-dependent expression of the lipid phosphatase SHIP. Nat. Cell Biol. *4*, 963–969.

Wang, J.W., Howson, J.M., Ghansah, T., Desponts, C., Ninos, J.M., May, S.L., Nguyen, K.H., Toyama-Sorimachi, N., and Kerr, W.G.

(2002). Influence of SHIP on the NK repertoire and allogeneic bone marrow transplantation. Science *295*, 2094–2097.

Ward, J.M. (1978). Pulmonary pathology of the motheaten mouse. Vet. Pathol. *15*, 170–178.

Webb, D.C., McKenzie, A.N., and Foster, P.S. (2001). Expression of the Ym2 lectin-binding protein is dependent on interleukin (IL)-4 and IL-13 signal transduction: identification of a novel allergy-associated protein. J. Biol. Chem. *276*, 41969–41976.

Weinstein, S.L., Finn, A.J., Dave, S.H., Meng, F., Lowell, C.A., Sanghera, J.S., and DeFranco, A.L. (2000). Phosphatidylinositol 3-kinase and mTOR mediate lipopolysaccharide-stimulated nitric oxide production in macrophages via interferon-β. J. Leukoc. Biol. *67*, 405–414.

Welch, J.S., Escoubet-Lozach, L., Sykes, D.B., Liddiard, K., Greaves, D.R., and Glass, C.K. (2002). T_H2 cytokines and allergic challenge induce Ym1 expression in macrophages by a STAT6-dependent mechanism. J. Biol. Chem. *277*, 42821–42829.

Williams, D.L., Li, C., Ha, T., Ozment-Skelton, T., Kalbfleisch, J.H., Preiszner, J., Brooks, L., Breuel, K., and Schweitzer, J.B. (2004). Modulation of the phosphoinositide 3-kinase pathway alters innate resistance to polymicrobial sepsis. J. Immunol. *172*, 449–456.

Wu, G., and Morris, S.M., Jr. (1998). Arginine metabolism: nitric oxide and beyond. Biochem. J. *336*, 1–17.

Zimmermann, N., King, N.E., Laporte, J., Yang, M., Mishra, A., Pope, S.M., Muntel, E.E., Witte, D.P., Pegg, A.A., Foster, P.S., et al. (2003). Dissection of experimental asthma with DNA microarray analysis identifies arginase in asthma pathogenesis. J. Clin. Invest. *111*, 1863–1874.